

APPLICATION OF POTENTIAL FLOW METHODS TO SHIP SQUAT IN DIFFERENT CANAL WIDTHS

T Gourlay, Curtin University, Australia

E Lataire, Ghent University, Belgium

G Delefortrie, Flanders Hydraulics Research, Belgium

SUMMARY

This paper presents a comparison of numerical methods with model test results for squat (sinkage and trim) of a 1:75 KVLCC2 model in the Flanders Hydraulics Research towing tank, at a range of rectangular canal widths and depths. The numerical methods are the *Linear-2D* and *Nonlinear-1D* methods in *ShallowFlow*, the *Double-Body* method in *HullWave* and the *Rankine-Source* method in *GL Rankine*. Analysis of the model tests showed that in the narrowest canals, mass flux past the ship was not conserved, nevertheless it appears that the *Nonlinear-1D* method may give good results for the narrowest canals. The *Linear-2D* method was found to give good results in the widest canal, particularly at the shallowest water depth. The *Rankine-Source* method was found to give good results for the widest canal, particularly at high speed. The *Double-Body* method was found to give quite consistently good results across all conditions.

NOMENCLATURE

AP	Aft perpendicular
B	Ship beam (m)
$b(x)$	Local ship waterline breadth (m)
C_B	Block coefficient based on L_{PP} (-)
F_h	Froude depth number (-)
FP	Forward perpendicular
g	Gravitational acceleration = 9.806 m/s ²
h	Water depth (m)
L_{PP}	Length between perpendiculars (m)
r	Radial distance from source (m)
$S(x)$	Local ship cross-section area (m ²)
s_{mid}	Midship sinkage (m)
T	Ship draft (m)
U	Ship speed (m/s)
w	Rectangular canal width (m)
X	=0 at start of canal test section, positive in direction of ship travel
x	=0 at transom, positive forward (m)
y	=0 on centreline, positive to port (m)
z	=0 at keel, positive upward (m)
λ	scale factor (-)

1 INTRODUCTION

Ships operate in different types of shallow-water areas where they are at risk of grounding due to squat, heel and wave-induced motions. Shallow-water areas might be open shallow water (such as Torres Strait), dredged channels (such as most approach channels across continental shelves) or canals with surface-piercing banks (such as river ports or inland waterways). The main focus of this paper is to work towards being able to predict ship squat accurately in any bathymetry.

Model tests are necessarily conducted in tanks with surface-piercing banks, so that dredged channels and open water cannot be simulated at model scale. For these cases, ideally a numerical method is used that has been validated against model test data in more restricted water-

ways. Typically the numerical method may be a potential flow method, a Computational Fluid Dynamics (CFD) method, or an empirical method. In this paper four potential flow numerical methods are considered.

The model test program considered here is unique in providing comprehensive measured squat results at six different canal widths. These model test results are ideal for validating numerical methods over a range of canal widths. The tests were done in a simple rectangular cross-section, which is realistic for locks, but not for river ports or inland waterways. Therefore numerical methods should also be assessed against model test results with realistic sloping bank conditions, such as [12, 15].

2 MODEL TESTS

2.1 EXPERIMENTAL PROGRAM

The hull considered here for model tests and numerical analysis is the KVLCC2 hull [8, 13]. This research hull, developed by Korea Research Institute of Ships and Ocean Engineering (KRISO) is representative of a Very Large Crude Carrier (VLCC).

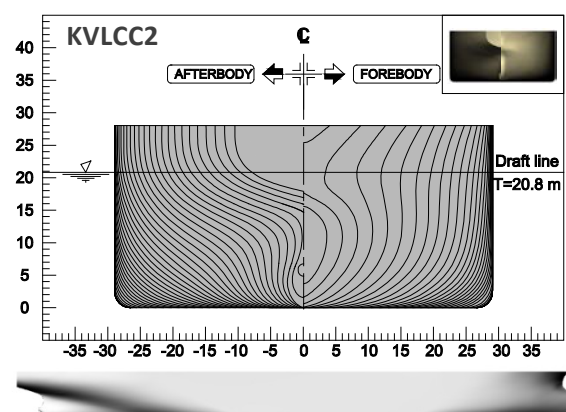


Figure 1. Body plan (top) and profile (bottom) of KVLCC2 hull

Model tests were undertaken in June 2010 in the Towing Tank for Manoeuvres in Shallow Water (cooperation Flanders Hydraulics Research — Ghent University) [1] on a 1:75 scale model of the KVLCC2. The tests are described in [9]. Principal particulars of the model and full-scale hull are shown in Table 1.

Table 1. Principal particulars of the KVLCC2 hull at model-scale and full-scale

	Model-scale	Full-scale
λ	75.0	1.0
L_{PP}	4.267m	320.0m
B	0.773m	58.0m
T	0.277m	20.8m
C_B	0.810	0.810

The towing tank has a length of 88m and width of 7.00m. This width is 9.05 times the model beam (i.e. $w/B=9.05$). By using a 30m-long vertical wall parallel to the tank walls, this width could be reduced to simulate successively narrower rectangular canals. At each canal width, various water depths were tested, as shown in Table 2.

Table 2. Model test combinations of canal width and water depth

Canal parameter	Values model-tested
w/B	1.05, 1.25, 1.70, 2.50, 5.00, 9.05
h/T	1.05 (only for $w/B=1.05$) 1.10, 1.35, 1.50 (all widths)

A range of ship speeds was undertaken for each canal configuration, as described in [9].

2.2 WAVE PROFILE OBSERVATIONS

The ship model was towed at a constant forward speed in the rectangular cross sections at different widths and water depth combinations (Table 2, Figure 2). At sub-critical speed conditions the water displaced by the sailing vessel has to flow under and along the vessel. This results in a return flow directed opposite to the sense of the motion of the vessel. A consequence of this return flow is a high flow velocity relative to the ship and hence a low pressure region on the ship's hull (Bernoulli's principle) which results in a decrease of the water level around the vessel. This is the cause of the running sinkage (or squat).

Based on the conservation of mass, the lower the water depth and/or the smaller the canal width the faster this return flow will be. However, the canal was open at both inlet and outlet, so water from the outer section could

freely flow in and out of the test section during a test run. This was specifically observed for the most confined cross sections, in which the full ship model acts like a piston, pushing the water out of the canal section. This effect has previously been observed and predicted by potential-flow theory at high speed [5], but in this case it appears that it may be affected by boundary-layer friction. The resulting wave system travels towards the far end of the towing tank, reflects and enters the test section again. The assumption of a mass conservation within the smaller cross section is no longer valid.



Figure 2. KVLCC2 model during an experiment.

During the model tests five wave gauges registered the water surface at five discrete positions in the towing tank (Figure 3). Two at the longitudinal centre of the installed rectangular cross section, one at starboard (wave gauge 1) and the other at port side (wave gauge 5) of the ship. Two wave gauges were positioned at the outlet of the test section, of which one was in the extended test section (wave gauge 4) and the other behind the starboard side wall (wave gauge 2). The final wave gauge was positioned in the extension of the centreline of the installed cross section but 15m away from the outlet (wave gauge 3).

The wave registrations at these wave gauges will be compared for five model tests. All tests are carried out at the same forward speed (6 knots full scale) and at the same water depth ($h=1.50T$). This water depth was selected because of the large availability of test results, however the observations are valid for all water depths tested. The lateral position of the ship model was always on the centreline of the installed cross section.



Figure 3. Positions of the wave gauges in the towing tank

The registration of the wave gauges 1 and 5 are plotted to the longitudinal position of the midship of the ship model in the cross section in Figure 4. Different observations can be made. The first peak of the water level (X is about 7m) is caused by the acceleration of the ship model. This acceleration results in a leading wave running through the tank at the critical speed. The wave height increases with decreasing canal width. After this wave has passed the wave gauges, the water level returns to its initial position ($X=15$ m) and when the ship passes wave gauges 1 and 5 a clear water level drop is visible ($17\text{m} < X < 21\text{m}$) which results in the squat of the ship. When the ship has passed, the water level returns to the initial water level except for the two smallest test sections ($w=1.25B$ and $1.05B$). For the latter the water level in the cross section is lower than the initial water level for a longer period of time.

The wave registration at the outlet of the test section (Figure 5) shows again the water level increase because of the acceleration of the ship model ($5\text{m} < X < 15\text{m}$) but there is a second, longer water level increase when the ship is at position $X=20\text{m}$ until the ship is at the end of the installed section ($X=33\text{m}$). This is caused by the previously described piston effect caused by the ship. The more confined the cross section the more water is pushed out and the higher the water level increases. This is almost absent in the $5.00B$ wide cross section but easily discernible in all the smaller cross sections. The ship only decelerates when it is entirely out of the installed cross section and as such the water level drop when she passes the wave gauges is again clearly visible ($33\text{m} < X < 37\text{m}$).

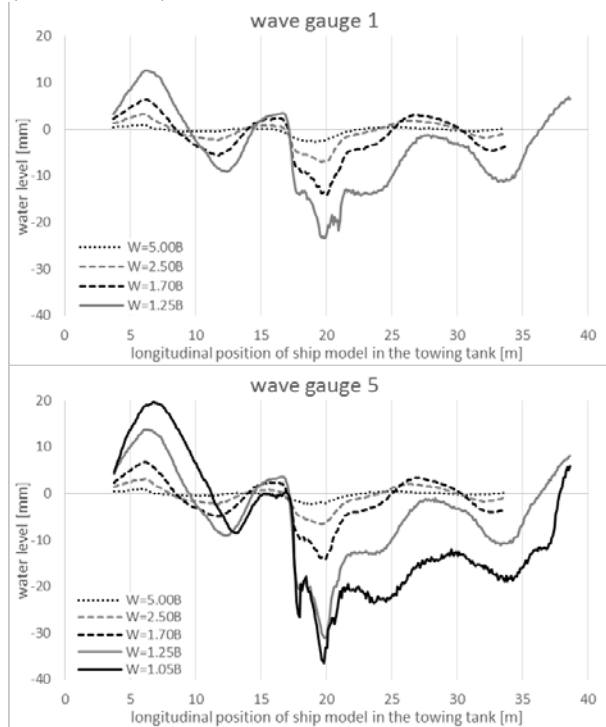


Figure 4. Wave registrations for two wave gauges at 5 different cross section widths

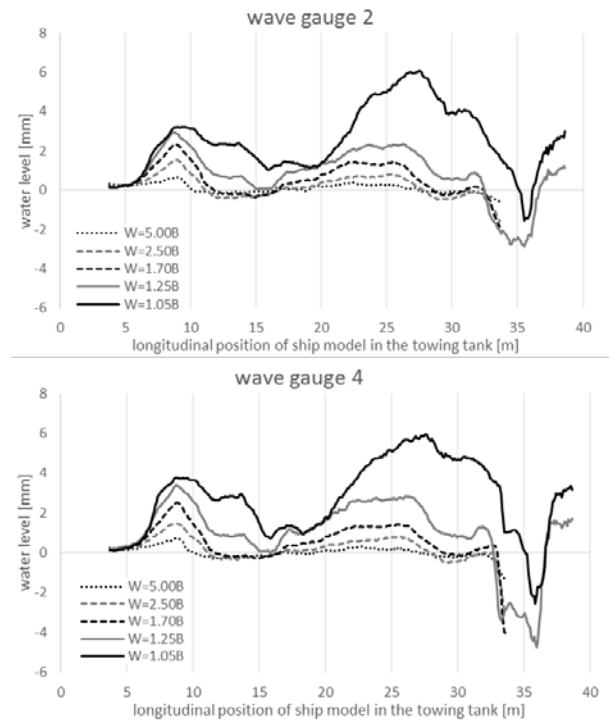


Figure 5. Wave registrations for two wave gauges at the outlet of five different cross section widths

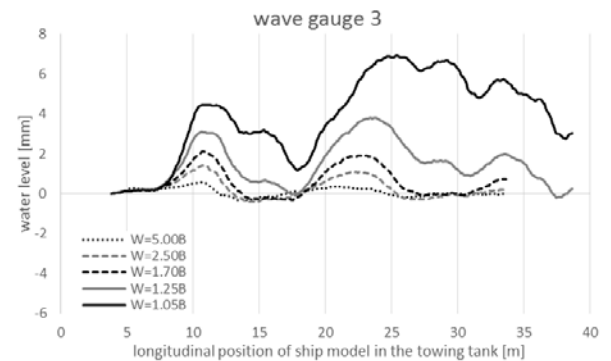


Figure 6. Wave registrations at the open section of the towing tank

Wave gauge 3 is positioned further away from the test section under consideration and the ship model stopped long before it reaches this gauge. In Figure 6 the water level increase because of the acceleration phase can be observed again ($8\text{m} < X < 15\text{m}$). From $X=18\text{m}$ a water level increase is observed which can be linked to the piston effect. This results in a long wave because the water level increases while the ship model is travelling through the canal section and at the same time pushing water out of the canal section. If the water level would have been measured for a longer period of time (after the model test terminated) then a water level drop would be observed. This long wave bounces back at the end of the towing tank and enters the cross section at the outlet again. Obviously, after some time the water level in the entire tank returns to its initial level.

3 NUMERICAL METHODS

3.1 LINEAR-2D METHOD

The *Linear-2D* method is the slender-body shallow-water theory of Tuck for rectangular canals [14]. Each hull cross-section is represented by a vertical line source with source strength proportional to the rate of change of section area, as shown in Figure 7.

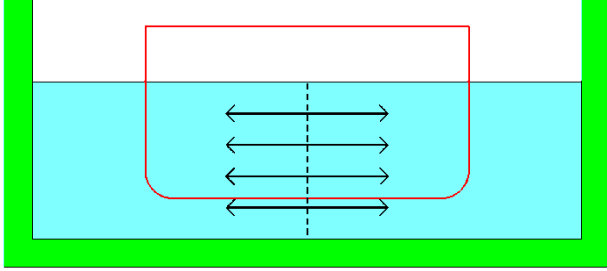


Figure 7. *Linear-2D* method. Each hull section is represented as a vertical line source, with strength proportional to the rate of change of section area.

The wall boundary conditions on the outside of the canal are correctly applied, but the method does not take account of the nonlinear blockage effect of the ship in the canal. The sources are assumed to lie on the hull centreline, rather than on the outside of the ship as done in the panel methods.

Flow speeds are averaged in the vertical direction, incorporating the shallow-water assumption. Therefore this is a two-dimensional method, with flow speeds varying longitudinally and transversely. The slender-body assumption is that ship beam and draft are small relative to ship length. This infers that flow disturbance velocities are small relative to the ship speed, and free surface slopes are small. Quadratic and higher-order terms in disturbance velocities and free-surface slope are therefore neglected. The method is implemented in the CMST in-house code *ShallowFlow*, as described in [4].

For this and the other methods, all calculations were done at full scale. Since potential-flow methods were used, there is no scale effect on any of the dimensionless output quantities.

An IGES file of the KVLCC2 was obtained from the SIMMAN workshop [13]. This was imported into MAXSURF software and used to develop offsets at 50 evenly-spaced sections from the transom to the front of the bulb, and 11 evenly-spaced waterlines from the keel to the design waterline. The hull offsets are shown in Figure 8.

ShallowFlow uses hull section areas and waterline breadths as input. Section areas were calculated using Simpson's rule, with correct treatment of the bilge radius

along the parallel midbody. Section areas and waterline breadths used for the KVLCC2 are shown in Figure 9.

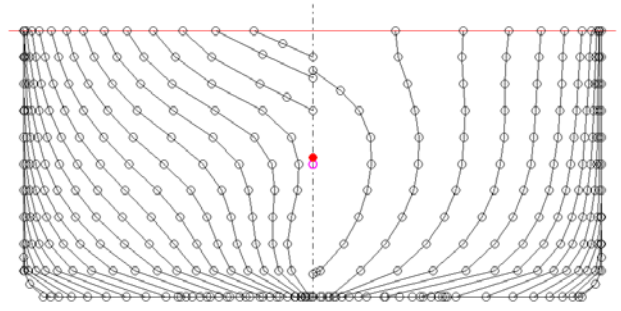


Figure 8. KVLCC2 offsets (circles) used to develop *ShallowFlow* and *HullWave* hull files

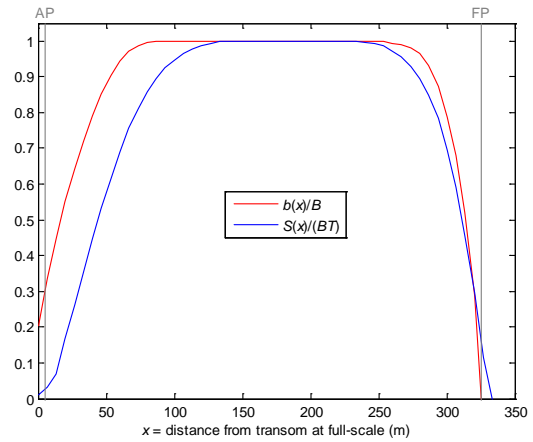


Figure 9. Section area and waterline breadth curve for KVLCC2, as input to *ShallowFlow*

All run times given here were on an Intel i7-940 2.93 GHz processor with 12 GB of RAM. Run time for the Linear 2D method was 3.8s to do a total of 200 speeds for a single bathymetry.

3.2 NONLINEAR-1D METHOD

The *Nonlinear-1D* method is the hydraulic theory described in [6], designed for narrow canals. This solves the mass conservation and Bernoulli equations, with constant flow velocity assumed across each canal cross-section, as shown in Figure 10.

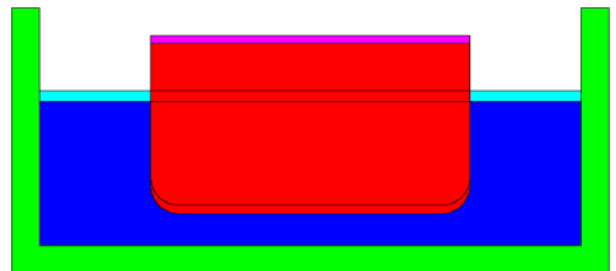


Figure 10. *Nonlinear-1D* method. Pink shows static floating position, red shows squatted position. Light blue shows static free surface, dark blue shows actual free surface.

Horizontal and vertical velocity components are neglected, and the longitudinal flow velocity is assumed constant across each cross-section. The water cross-section area (dark blue area shown in Figure 10) is calculated allowing for the squat of the ship and the changed free surface height, approximating the ship as wall-sided at the waterline. Therefore this is a one-dimensional, but highly nonlinear, method.

The *Nonlinear-1D* method is implemented in *Shallow-Flow* and uses the same hull input files as the *Linear-2D* method described above. Run time for this method was 292s to do a total of 200 speeds for a single bathymetry.

3.3 DOUBLE-BODY METHOD

The *Double-Body* method is developed in this article. It is an extension of the method commonly used for ships in deep water, and less commonly for ships in shallow open water.

For a ship in deep water, the double-body method involves reflecting the submerged ship hull about the static free surface, so as to model the free surface as a rigid wall, as shown in Figure 11.

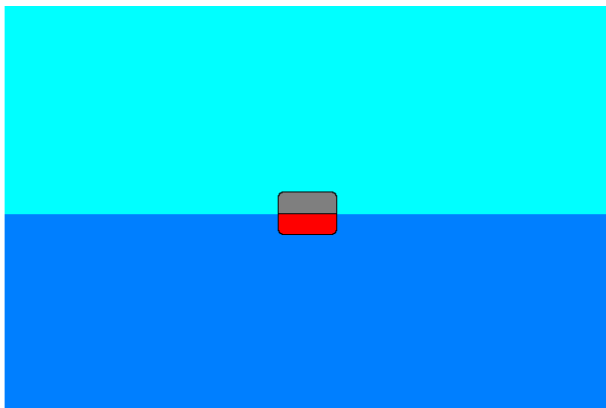


Figure 11. Double-body method for a ship in deep water (stern view). Submerged hull shown in red, image hull shown in grey.

The double-body method is commonly used to approximate the flow field around ships at low speed in deep water. The approximation can be exploited in model testing, by using a double-body of the ship in a recirculating water flume or wind tunnel (see e.g. [10]).

For a ship in open shallow water a double-body method using an infinite vertical array of ship reflections was developed [11], as shown in Figure 12. In this article the method is extended to model a ship in a shallow canal with vertical walls, by using an infinite array of horizontal and vertical reflections, as shown in Figure 13.

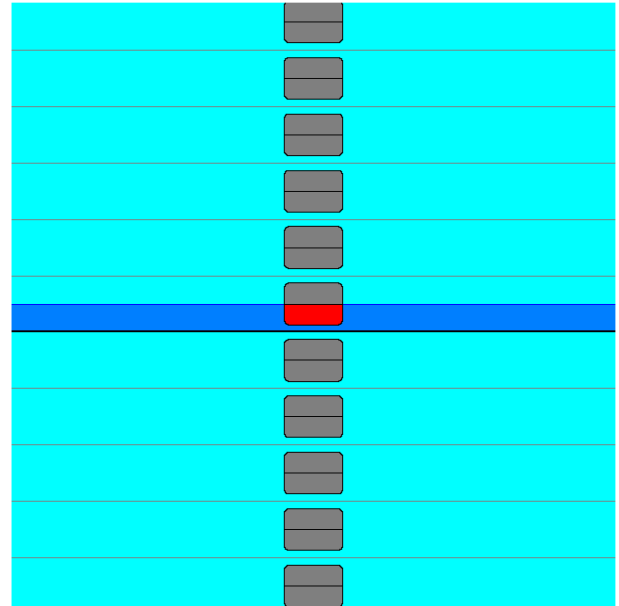


Figure 12. Double-body method for a ship in shallow open water (stern view). Submerged hull shown in red, image hulls shown in grey.

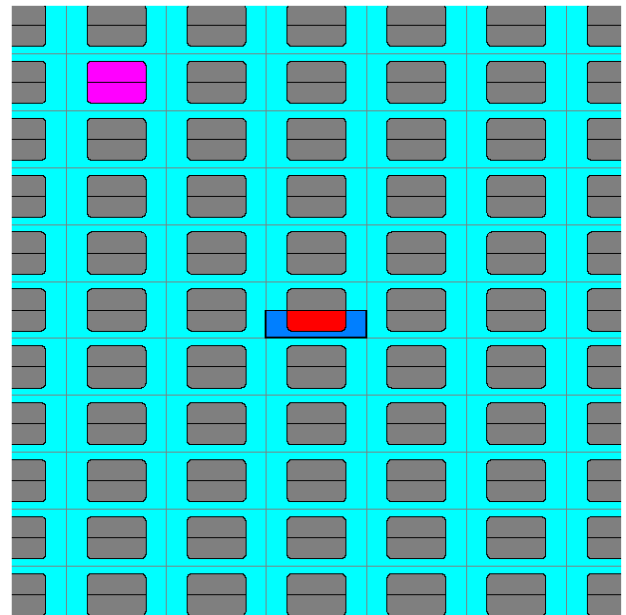


Figure 13. Image system stretching to infinity for ship in a shallow rectangular canal (stern view). Submerged hull shown in red. Image hulls shown in grey. Example image hull shown in pink as used in Figure 15.

Other than the horizontal reflections, the analysis goes over unchanged from that described in [11]. A standard Hess and Smith panel method [7] is used, implemented in CMST's submarine hydrodynamics code *HullWave* [2]. Although *HullWave* is written to model Havelock sources, it can be run in Rankine source mode by removing the Havelock free-surface correction terms.

HullWave requires a hull surface mesh as input. Because of the computational intensity of the *Double-Body* meth-

od, a relatively coarse mesh of 868 panels was used, as shown in Figure 14. Convergence testing showed that sinkage and trim were well-converged with this number of panels.

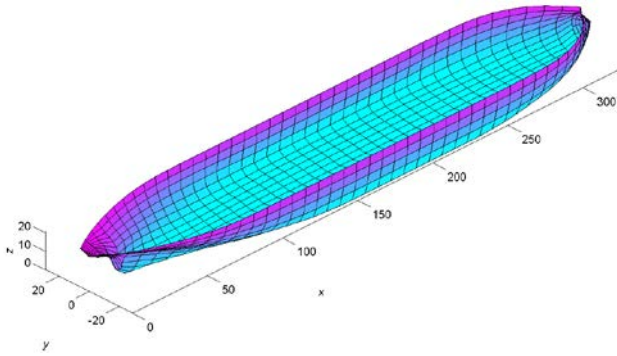


Figure 14. 868-panel surface mesh (434 panels port side) used for *HullWave* calculations. Hull meshed up to static waterline.

Each hull panel is considered to be a source of uniform source density. The wall boundary condition is applied at the null point of each panel, as described in [7]. This includes contributions from the submerged hull as well as all of the hull reflections shown in Figure 13 (theoretically out to infinity). For the meshed hull shown in Figure 14, this results in a 434×434 matrix equation for the 434 unknown source densities on the port side of the hull.

The method was tested first in shallow open water (Figure 12), where it was found to agree with [14] for a slender hull, and give slightly higher sinkage than [14] for the KVLCC2 hull, as expected. Convergence was rapid with vertical reflections for the shallow-open-water case.

For the shallow-canal case, convergence is slower and can be assessed as follows. Consider the radius vector from an image source panel to a hull receiver panel, as shown in Figure 15.

Due to the symmetry, transverse and vertical velocity contributions from diagonally opposite hull images quickly tend to cancel out for distant hull images. No such cancellation occurs for longitudinal velocities, due to the ship's fore-aft asymmetry. Radial velocities are $O(1/r^2)$, so longitudinal velocities are $O((1/r^2)(L_{pp}/r))$. Summing the contributions from all hull images is $O((1/r^2)(L_{pp}/r)(2\pi r dr))$, which is convergent as $r \rightarrow \infty$.

Run time for the *Double-Body* method was 25 minutes for a single bathymetry. A single run gives the results for all speeds, due to the quadratic speed dependence.

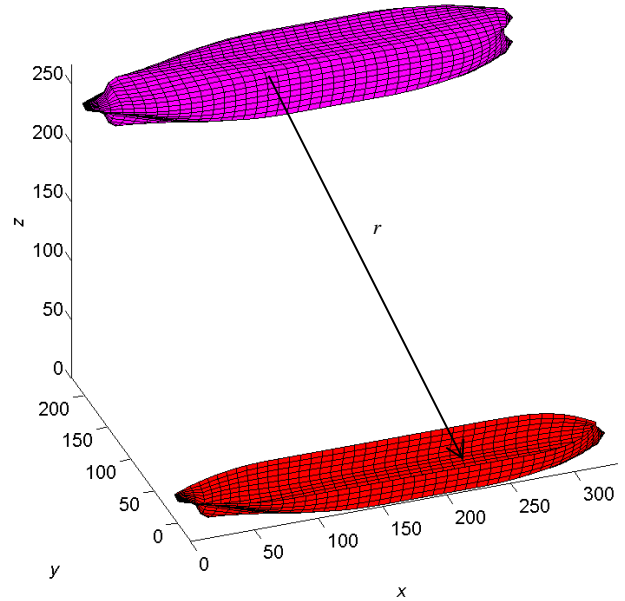


Figure 15. Radius vector from source panel on image hull (pink) to receiver panel on actual submerged hull (red), distance r . See also Figure 13.

3.4 RANKINE-SOURCE NUMERICAL METHOD

The *Rankine-Source* method is implemented in *GL Rankine* [16] using Rankine source patches on the hull and free surface, and exact hull and free-surface boundary conditions.

GL Rankine uses an input STL file and automatically generates a hull surface mesh, based on input mesh size parameters. The surface mesh generated by *GL Rankine* and used for these calculations is shown in Figure 16.

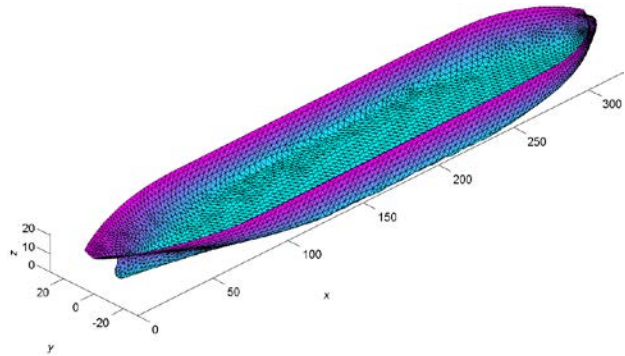


Figure 16. 7936-panel surface mesh (3968 panels port side) used for *Rankine-Source* calculations. Hull meshed up to static waterline.

These calculations were run by CMST under an academic license supplied by DNV GL. Run times were in the order of 1 minute for each ship speed in each bathymetry.

4 RESULTS AND DISCUSSION

Comparisons between the four potential-flow methods and model test results are shown in Appendix A for midship sinkage and Appendix B for dynamic trim. Ship speed is non-dimensionalized using the Froude depth number:

$$F_h = \frac{u}{\sqrt{gh}} \quad (1)$$

Most of the model tests were done with propeller operating at the self-propulsion point (labelled “Self-prop.”). For $w/B = 9.05$, tests were also done with the propeller fixed (labelled “Towed”). We can see that the self-propelled model tends to have larger midship sinkage and less bow-down trim than the towed model, which is in line with comparisons for container ships [3].

Some of the tests involved very low speed, at which the Rankine-Source method has difficulty resolving the very short wavelengths produced. Therefore converged results for the Rankine-Source method could not be obtained in all cases. The other methods are shown for all cases.

As discussed in Section 2.2, mass flux past the ship was not conserved in the model tests for $w/B = 1.05$ and 1.25 . We see that measured trim is bow-up for these model tests, with water being pushed ahead of the ship and a wave trough trailing behind the ship. The numerical methods all assume conservation of mass flux past the ship, so these comparisons are not fair comparisons. Further numerical and/or experimental work are required in order to make fair comparisons between theory and experiment for the narrowest canals. Qualitatively speaking, we may say that the effect of having non-constant mass flux may be to cause a bow-up trim and decrease the sinkage. We may infer that the *Nonlinear-1D* method is likely to give the most accurate sinkage predictions for the narrowest canals.

For $w/B = 1.70$ and 2.50 , the *Nonlinear-1D* and *Double-Body* methods are close to the measured sinkage results, while the *Linear-2D* and *Rankine-Source* methods significantly under-estimate the sinkage. It was expected that the *Rankine-Source* results would be larger than the *Linear-2D* results and closer to the *Double-Body* results, so further work will be done in future on the *Rankine-Source* method in narrow canals. The ship-piston effect on the measured results is diminishing at this canal width, which results in a measured trim that changes sign, but which is still small compared to the numerical methods for $w/B = 1.70$.

The case $w/B = 5.00$ is the “cross-over” point for the *Linear-2D* and *Nonlinear-1D* methods. For narrower canals, the *Nonlinear-1D* method gives larger sinkage (because of the nonlinearity) and is closer to the model test results; for wider canals the *Linear-2D* method gives larger sinkage (because it predicts higher flow speeds near the ship) and is closer to the model test results. At

this canal width, all four potential methods give similar sinkage predictions, which under-estimate the measured sinkage at this canal width. The *Linear-2D* and *Double-Body* methods give similar trim predictions, which are very close to the measured results for $F_h < 0.4$, but under-predict at higher speeds. The *Rankine-Source* method gives generally larger bow-down trim than the *Double-Body* and *Linear-2D* method here, and is further from the model tests at $h/T = 1.10$ but closer at $h/T = 1.35$.

For $w/B = 9.05$, the *Linear-2D*, *Double-Body* and *Rankine-Source* methods all give similar sinkage for $F_h < 0.4$, and all are close to the model test results. The predictions are smaller than the self-propelled model results by 15%, 13% and 13% respectively at $F_h = 0.43$, and 21%, 22% and 16% respectively at $F_h = 0.50$. The *Rankine-Source* method again predicts larger bow-down trim than the *Linear-2D* and *Double-Body* methods. All of these methods give trim predictions which are close to the measured results, with differences comparable to the difference between towed and self-propelled models.

5 CONCLUSIONS

- An extensive set of model test results for the KVLCC2 has been used to validate four potential-flow methods over a range of rectangular canal widths and depths.
- The most restricted model tests showed that mass flux past the ship was not conserved, so that fair comparisons could not be made between the model tests and numerical methods. The effect was most noticeable on trim, because water builds up in front of the model, causing the bow to rise (this is also observed when entering a lock). Further numerical and/or experimental work are required to better understand this effect.
- Despite the above, it appears that the *Nonlinear-1D* method may give good estimates of midship sinkage in narrow canals ($w/B \leq 2.5$). It is inappropriate for wide canals with $w/B > 5.0$, due to the 1D assumption being violated.
- The *Linear-2D* method gives good results for wide canals with $w/B > 5.0$, although an empirical correction is desirable, especially at high speeds. This method is inappropriate for narrow canals with $w/B < 5.0$, due to the linear flow assumption being violated.
- The *Rankine-Source* method gives good results for wide canals, especially at higher speeds when the *Linear-2D* method under-predicts the midship sinkage. Unexpectedly-low sinkage results were obtained for the *Rankine-Source* method in narrow canals, and further work will be done on this topic.
- The *Double-Body* method gave quite consistently good results across all canal widths.

6 ACKNOWLEDGEMENTS

Alexander von Graefe provided assistance with installing, running and convergence testing GL Rankine software. Scott Ha provided assistance with KVLCC2 hull modelling.

7 REFERENCES

1. Delefortrie, G.; Geerts, S.; Vantorre, M. (2016). The Towing Tank for Manoeuvres in Shallow Water. *MASHCON 2016*, Hamburg, Germany.
2. Gourlay, T.P.; Dawson, E., (2015). A Havelock-source panel method for near-surface submarines. *Journal of Marine Science and Application* 15(3), 215-224.
3. Gourlay, T.P.; Ha, J.-H.; Mucha, P.; Uliczka, K. (2015). Sinkage and trim of modern container ships in shallow water. *Proc. Coasts and Ports*, Auckland, 15-18 September 2015.
4. Gourlay, T.P. (2014). ShallowFlow: A program to model ship hydrodynamics in shallow water. *Proc. 33rd International Conference on Ocean, Offshore and Arctic Engineering (OMAE 2014)*, June 8-13, San Francisco, USA.
5. Gourlay, T.P. (2001). The supercritical bore produced by a high-speed ship in a channel. *Journal of Fluid Mechanics* 434, 399-409.
6. Gourlay, T.P. (1999). The effect of squat on steady nonlinear hydraulic flow past a ship in a channel. *Schiffstechnik* 46, 217-222.
7. Hess, J.L.; Smith, A.M.O. (1964). Calculation of nonlifting potential flow about arbitrary three-dimensional bodies. *Journal of Ship Research* 8(2), 22-44.
8. Kim, W.J.; Van, S.H.; Kim, D.H. (2001). Measurement of flows around modern commercial ship hulls. *Experiments in Fluids* 31, 567-578.
9. Lataire, E.; Vantorre, M.; Delefortrie, G., (2012). A prediction method for squat in restricted and unrestricted rectangular fairways. *Ocean Engineering* 55, 71-80.
10. Lee, S.-J.; Kim, H.-R.; Kim, W.-J.; Van, S.-H. (2003). Wind tunnel tests on flow characteristics of the KRISO 3,600 TEU containership and 300K VLCC double-deck ship models. *Journal of Ship Research* 47(1), 24-38.
11. Martin, H.; Puls, D. (1986). Vertical forces, trim moments and changes of draught and trim of ships in shallow water. *Schiffbauforschung* 25(3), 155-159.

12. Mucha, P.; el Moctar, O. (2014). PreSquat - Numerische Vorhersagen von dynamischem Squat in begrenzten Gewässern, *Bericht F005/2014*, Institut für Schiffstechnik, Universität Duisburg-Essen.

13. SIMMAN 2014 (2014). Workshop on Verification and Validation of Ship Manoeuvring Simulation Methods, Copenhagen, Denmark, December 8 -10. www.SIMMAN2014.dk

14. Tuck, E.O. (1967). Sinkage and trim in shallow water of finite width. *Schiffstechnik* 14, 92-94.

15. Uliczka, K.; Kondziella, B.; Flügge, G. (2004). Dynamisches Fahrverhalten sehr großer Containerschiffe in seitlich begrenztem extremen Flachwasser, *HANSA*, 141.

16. von Graefe, A. (2014). A Rankine source method for ship-ship interaction and shallow water problems, *Ph.D. thesis*, University of Duisburg-Essen.

8 AUTHORS BIOGRAPHY

Tim Gourlay is a Senior Research Fellow at the Centre for Marine Science and Technology, Curtin University. He undertakes research and consulting work in ship under-keel clearance for ports in Australia and internationally. This work typically includes theoretical development, software development, UKC management guidelines, port liaison and full-scale validation trials.

Evert Lataire is currently assistant at the division of Maritime Technology at Ghent University. He has made a PhD on the topic of bank effects mainly based upon model tests carried out in the shallow water towing tank of FHR. His ten year experience includes research on ship manoeuvring in shallow and confined water such as ship-ship interaction, ship-bottom interaction and ship-bank interaction

Guillaume Delefortrie, naval architect, is expert nautical research at Flanders Hydraulics Research. He is in charge of the research in the Towing Tank for Manoeuvres in Shallow Water, development of mathematical models based on model tests and is secretary of the 27th and 28th ITTC Manoeuvring Committee.

APPENDIX A: MIDSHIP SINKAGE COMPARISONS

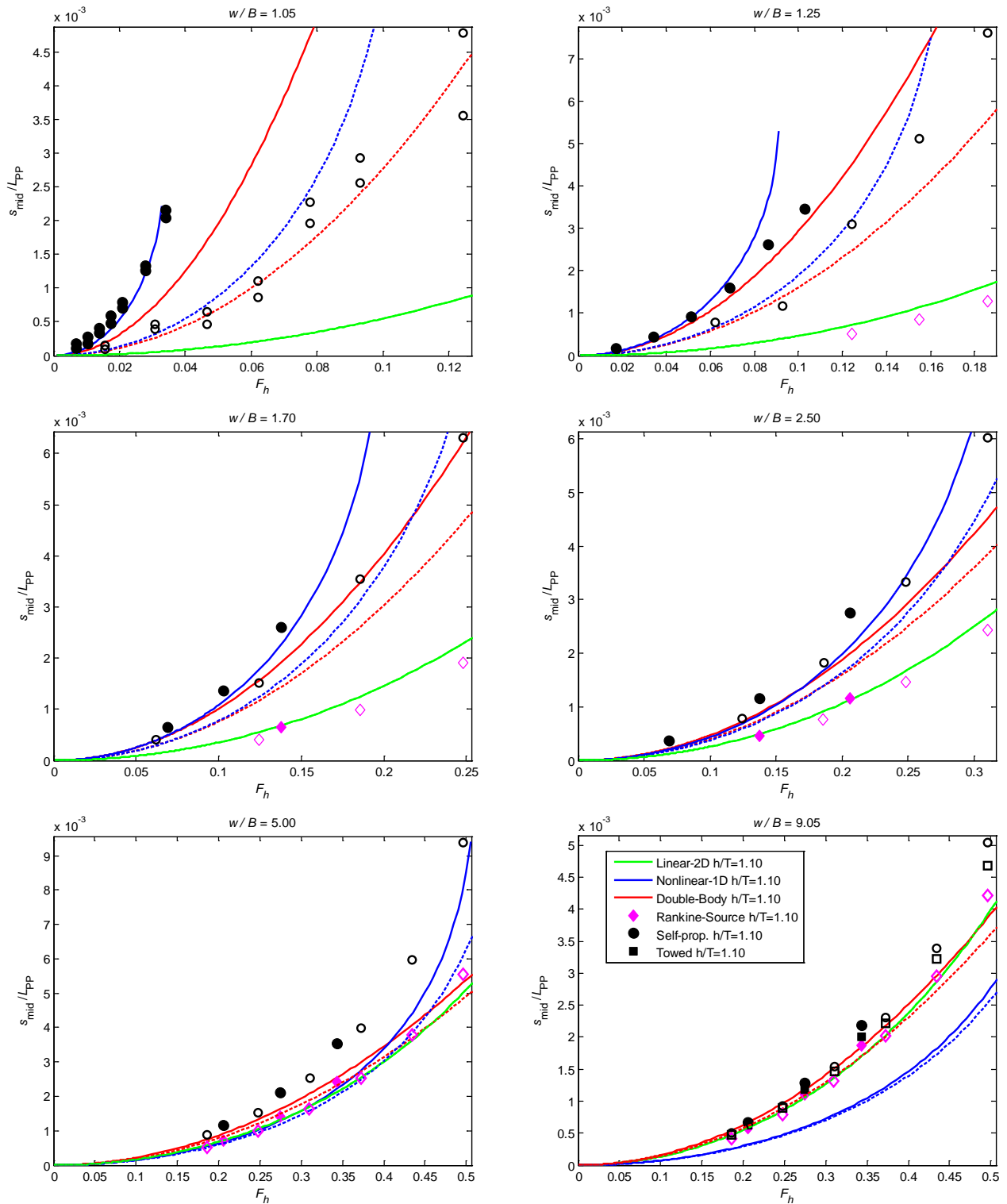


Figure A1. Midship sinkage predictions and model test results for KVLCC2 in rectangular canals of increasing w/B ratio. The same legend applies to all subplots. Dashed lines and unfilled markers are corresponding results for $h/T=1.35$. The *Linear-2D* results for both water depths are almost coincident.

APPENDIX B: DYNAMIC TRIM COMPARISONS

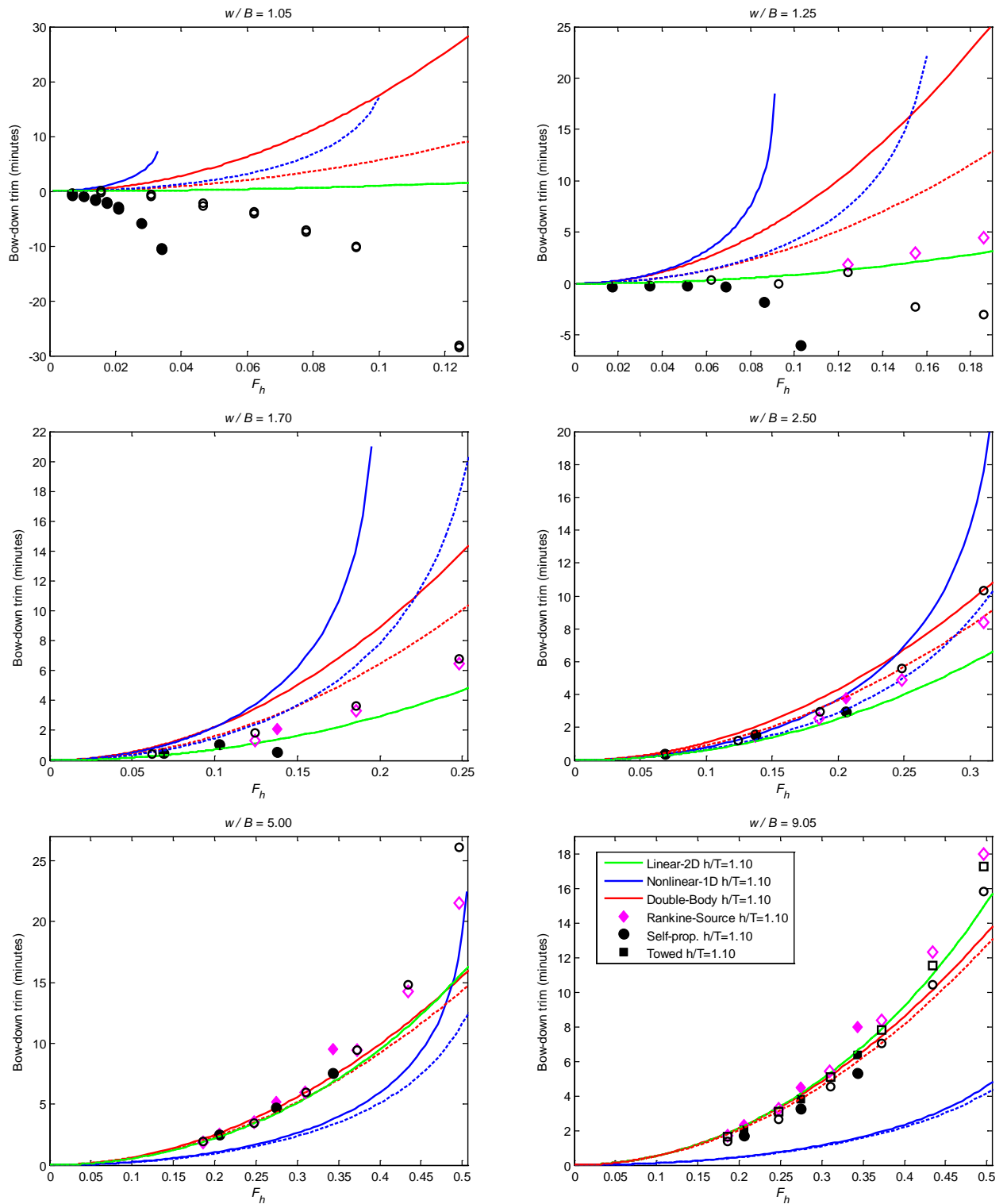


Figure B1. Dynamic trim predictions and model test results for KVLCC2 in rectangular canals of increasing w/B ratio. The same legend applies to all subplots. Dashed lines and unfilled markers are corresponding results for $h/T=1.35$. The *Linear-2D* results for both water depths are almost coincident.